

Published in final edited form as:

Chembiochem. 2008 November 24; 9(17): 2872–2882. doi:10.1002/cbic.200800248.

Protein Farnesyltransferase Catalyzed Isoprenoid Transfer To Peptide Depends On Lipid Size and Shape, not Hydrophobicity

Dr. Thangaiyah Subramanian[‡], Dr. Suxia Liu[‡], Dr. Jerry M. Troutman[‡], Prof. Douglas A. Andres^{‡,||}, and Prof. H. Peter Spielmann^{‡,§,||}

H. Peter Spielmann: hps@uky.edu

[‡]Department of Molecular and Cellular Biochemistry, University of Kentucky, Lexington, Kentucky 40536-0084

[§]Department of Chemistry, University of Kentucky, Lexington, Kentucky 40536-0084

^{||}Kentucky Center for Structural Biology, University of Kentucky, Lexington, Kentucky 40536-0084, Fax: (+)1-859-257-8940

Abstract

Protein farnesyl transferase (FTase) catalyzes transfer of a 15-carbon farnesyl group from farnesyl diphosphate (FPP) to a conserved cysteine in the C-terminal Ca₁a₂X motif of a range of proteins, including the oncoprotein H-Ras (“C” refers to the cysteine, “a” to any aliphatic amino acid, and “X” to any amino acid) and the lipid chain interacts with, and forms part of the Ca₁a₂X peptide binding site. Previous studies have shown that H-Ras biological function is ablated when it is modified with lipids three-to-five orders of magnitude less hydrophobic than FPP. Here, we employed a library of anilinoogeranyl diphosphate (AGPP) and phenoxygeranyl diphosphate (PGPP) derivatives with a range of polarity (logP (lipid alcohol) = 0.7–6.8, logP (farnesol) = 6.1) and shapes to examine whether FTase catalyzed transfer to peptide was dependent on the hydrophobicity of the lipid. Analysis of steady-state transfer kinetics for analogues to dansyl-GCVLS peptide revealed that the efficiency of lipid transfer was highly dependent on both the shape and size, but was independent of the polarity of the analogue. These observations indicate that hydrophobic features of isoprenoids critical for their association with membranes and/or protein receptors are not required for efficient transfer to Ca₁a₂X peptides by FTase. Furthermore, the results of these studies indicate that the role played by the farnesyl lipid in the FTase mechanism is primarily structural. We propose a model where the FTase active site stabilizes a membrane interface-like environment to explain these results.

Keywords

Protein Farnesyltransferase; Farnesyl diphosphate; Enzyme Catalysis; Lipophilicity; Terpenoids

Introduction

Protein farnesyl transferase (FTase) catalyzes transfer of a 15-carbon farnesyl group from farnesyl diphosphate (FPP, **1**, Figure 1) to a conserved cysteine in the C-terminal Ca₁a₂X motif of a range of proteins, including the oncoprotein H-Ras (“C” refers to the cysteine, “a”

Correspondence to: H. Peter Spielmann, hps@uky.edu.

Supporting information for this article is available on the WWW under <http://www.chembiochem.org> or from the author.

Supporting Information: Spectral data for **3**, **4**, **5**, **6a–6ad**, **7**, **14**, **15**, **18a–18c**, **19a–19c**, **24a–24ad**, **27a–27c**, **28a–28c**, **29a–29c**, **30a–30c**, **31a–31c**, **32a–32c**. ¹H spectra of **3**, **15**, **19a–d**, **24a–ad**, ¹H, ³¹P and LRMS spectra of **4**, **5**, **6a–6ad**, **7**, **9a–9c** are available.

to primarily aliphatic amino acids, and “X” to any amino acid). Farnesylation is obligatory for the proper biological function of H-Ras and a number of small molecule inhibitors of FTase (FTIs) have been developed as anti-cancer agents.^[1–5] Several FTIs are currently in phase I, II and III clinical trials for the treatment of cancer,^[2, 6–7] but the response in patients has not been significant.^[1] An explanation for the lack of FTI clinical efficacy is the process of alternative prenylation where some FTase substrates can become geranylgeranylated by geranylgeranyl transferase type I (GGTase-I) when FTase activity is limiting.^[1, 8–10] This has led to substantial interest in developing alternative lipids incapable of supporting normal prenyl group function.^[11–13] Several studies have examined lipid features that influence the efficiency of isoprenoid transfer to Ca₁a₂X peptides by FTase.^[13–19] These studies have focused on how the length of the isoprenoid affected transfer kinetics,^[14] replacing the terminal isoprene with aryl substituents,^[15, 18, 20–21] and altering the steric demands and electronic properties of the isoprenoid branched methyl groups.^[13–14, 16, 22–23] Despite these efforts, information on the structural features that give rise to productive interactions of FPP analogues with the FTase active site remain limited. The reaction mechanism of FTase is unexpectedly complex (Figure 2). Product release is the rate determining step (k_{cat}) for the FTase reaction, and an unusual feature of the FTase mechanism is that product dissociation is greatly enhanced by binding of either a new FPP or Ca₁a₂X peptide substrate. Remarkably, the hydrophobic thioether product has decreased affinity for the enzyme despite the non-polar amino acid residues lining the active site.^[24] X-ray crystallographic analysis shows that the lipid chain interacts with, and forms a substantial part of the Ca₁a₂X peptide binding site throughout the course of the reaction.^[25–26]

FPP analogues have been used to study the physical interactions between the lipid, FTase and the Ca₁a₂X peptide as well as the biological function of the modification.^[12, 15–16, 18, 27] The Ca₁a₂X tetrapeptide is sufficient for prenyltransferase recognition, and the kinetics of FPP transfer to dns-GCVLS is identical to that of full length H-Ras.^[28–29] The analogue 8-anilino geranyl diphosphate (AGPP, **2a**, Figure 1) is transferable to Ca₁a₂X substrates with apparent steady-state kinetics nearly identical to FPP, and the aniline moiety appears to act as an isostere for the FPP terminal isoprene.^[15, 20] AGPP has been used to probe the endogenous modification of proteins by FTase and is competitive with FPP *in vitro* and in cell culture.^[20, 30–31] We previously prepared and examined the FTase catalyzed lipid transfer of an AGPP analogue library to the dns-GCVLS peptide corresponding to the H-Ras Ca₁a₂X motif and found that reactivity depends on both size and shape of the lipid.^[32–33] Small *meta*- and *para*-substitutions on the aniline ring increase reactivity with dns-GCVLS while others with *ortho*-substitutions were potent dns-GCVLS modification FTase inhibitors. In other work, investigation of ten FPP analogues showed that the normal biological function of H-Ras is blocked when modified with isoprenoids that are three-to-five orders of magnitude less hydrophobic than the farnesyl group.^[12] H-Ras biological function appears to require a minimum lipophilicity of the prenyl group to allow important interactions downstream of the C-terminal processed H-Ras protein. These observations suggest that hydrophilic FPP analogues are prenyl function inhibitors (PFIs) that may serve as lead compounds for a unique class of potential anti-cancer therapeutics. However, the poor reactivity of the least polar FPP analogue Isox-GPP, **8** with H-Ras and Ca₁a₂X peptides raised the possibility that other polar FPP analogues might also be poor substrates for FTase.

The anti-Ras behavior of this small set of more polar FPP analogues prompted us to examine the relationship of isoprenoid hydrophobicity to the efficiency of FTase catalyzed lipid transfer to Ca₁a₂X peptides. Additional FPP analogues with a range of polarity and shapes were prepared and their transfer efficiency determined. We found that the efficiency of lipid transfer was highly dependent on both the shape and size, but was independent of the hydrophobicity of the analogue. The apparent catalytic efficiency ($k_{\text{cat}}/K_{\text{m}}^{\text{peptide}}$) for transfer of several analogues to a dns-GCVLS (H-Ras Ca₁a₂X sequence) peptide was greater

than that for the natural substrate FPP. These observations indicate that hydrophobic features of isoprenoids critical for their association with membranes and/or protein receptors are not required for efficient transfer to Ca₁a₂X peptides by FTase, and that hydrophobic interactions between the lipid and aromatic residues in the FTase active site do not drive binding of FPP to the enzyme. Furthermore, the results of these studies indicate that the role played by the farnesyl lipid in the FTase mechanism is primarily structural. We propose a model where the FTase active site stabilizes a membrane interface-like environment to explain these results.

Results and Discussion

Synthesis of FPP analogues where the AGPP amino group is replaced by other moieties

In order to examine whether the AGPP aniline nitrogen contributed specific interactions obligatory for efficient analogue transfer to Ca₁a₂X peptides, molecules **3**, **4**, **5**, **6a** and **7** with CH₂, S, CH₂O, O linkers between the terminal aryl group and the geranyl chain were synthesized. Methylene linked analogue **3** was prepared in five steps from 8-chlorogeranyl acetate using a modified procedure of Spencer and co-workers (Scheme 1).^[34] THP ether **13** was obtained by protection of 8-chlorogeraniol **12** in quantitative yield. Coupling of benzyl magnesium chloride with chloride **13** followed by removal of the THP ether provided alcohol **15** which was converted to the corresponding bromide and diphosphorylated to give diphosphate **3**.

The key step in the preparation of analogues **4**, **5** and **7** was alkylation of the appropriate, thiophenol or benzylalcohol with 8-bromogeranyl acetate **16** (Scheme 2). The desired diphosphates **4**, **5** and **7** were then obtained by saponification of acetates **18a–c** to give alcohols **19a–c** which were converted to the corresponding bromides followed by diphosphorylation with (Bu₄N)₃HP₂O₇ in CH₃CN. Compound **6a** was prepared by solid state Mitsunobu reaction as described below.

Analogue linker atom has a moderate effect on reactivity with Ca₁a₂X peptide

The kinetic parameters $^{app}k_{cat}$, and $^{app}K_m^{peptide}$ for analogue transfer to dns-GCVLS were measured utilizing a continuous fluorescence assay. The apparent $k_{cat}/K_m^{peptide}$ is the catalytic efficiency of FTase which measures the ability of the enzyme to catalyze a reaction at low peptide substrate concentrations. We found that the linker appears to have only a modest effect on the transfer efficiency, suggesting that the aniline nitrogen is not critical for efficient transfer of the unsubstituted parent molecules. Consistent with previous observations, transfer of the bulky 3,4,5-trimethoxy substituted analogue **7** was not detected. All reactions between FPP analogues and dns-GCVLS peptide were analyzed by HPLC with detection of the resulting components by dansyl fluorescence. No product detected by HPLC where we observe no increase in dansyl fluorescence. Although single turnover reactions for the "non-reactive" analogue diphosphates can not be excluded by this method, the lack of steady state turnover indicates that product release is impaired.

Synthesis of phenoxygeranyl diphosphate FPP analogue library

A library of 25 transferable AGPP derivatives had been previously prepared.^[35–36] The number of analogues to be examined was increased by preparing a directed library of 33 ether linked phenoxygeranyl diphosphates (PGPP) **6a–ad** and **9a–c** (Scheme 3 & 4). The PGPP ether linkage removes the aniline H-bond donor, alters the conformational preference of the lipid and allows for the straightforward introduction of polar functional groups. A focused phenoxygeranyl diphosphate library was prepared by a mixed solid-phase organic synthesis (SPOS)-solution phase route (Scheme 3). Reduction of the previously described resin-bound aldehyde **20** with NaBH₄ in DCE/EtOH (1:1) furnished the corresponding

alcohol **21** in 82% yield. Diversity was introduced into the library by solid phase Mitsunobu reaction of alcohol **21** with 5 equivalents of the appropriately substituted phenols in DCE at room temperature to provide the corresponding resin bound ethers **23a–ad**. The resin bound THP ethers **23a–ad** were released from the resin as the corresponding allylic bromides by agitation with two equivalents of Ph_3PBr_2 in CH_2Cl_2 for 4 h and the bromides were then trapped in situ with 6 equivalents of $(\text{Bu}_4\text{N})_3\text{HP}_2\text{O}_7$ in CH_3CN to give the desired phenoxygeranyl diphosphates **6a–ad**. The crude diphosphates were converted to the NH_4^+ form by ion exchange chromatography and then purified by RP-HPLC. Release of the THP resin linked lipids as the corresponding allylic bromides provides a traceless linker pathway to the desired FPP analogues **6a–ad**. The phenoxygeraniols **24a–ad** were made by cleavage of ethers **23a–ad** from the resin by treatment with DCE/MeOH/PPTS at 80°C followed by silica gel column chromatography (Table 2).

Three additional hydroxymethyl PGPP derivatives **9a–c** were prepared by solution methods (Scheme 4) to test the hypothesis that the size and shape of the lipid rather than the absolute polarity are essential for efficient transfer by FTase to peptide. AGPP analogues with methoxy, trifluoromethoxy and ethyl groups are transferred to dns-GCVLS by FTase^[32] and the polar hydroxymethyl group is roughly isosteric with these moieties (Scheme 4). Preparation of these polar PGPP analogues required masking of the reactive hydroxymethyl group during synthesis. The similar reactivity of the benzylic and allylic alcohol functions as well as the acid and base sensitive diphosphate in these amphipathic molecules narrowly constrain suitable protecting groups that can be used. Consequently, we employed the photolabile α -methyl-*o*-nitrobenzyl carbonate group to protect the hydroxymethyl group of analogues **28a–c** during THP cleavage, subsequent diphosphorylation, ion exchange and purification. Alcohols **29a–c** were obtained by Mitsunobu reaction of 8-hydroxy-OTHP protected geraniol **25** with either 3- or 4-hydroxybenzaldehyde or methylsalicylate followed by NaBH_4 reduction. The THP protected alcohols **28a–c** were acylated with α -methyl-*o*-nitrobenzyl chloroformate to give carbonates **30a–c**. The corresponding isoprenoid alcohols **31a–c** were obtained in quantitative yield by cleavage of THP ethers **30a–c** with PPTS in MeOH. The nitrobenzyl protected diphosphates **32a** and **32c** were obtained by treating the alcohols **31a–c** with Ph_3PBr_2 to give the corresponding bromide which were then trapped in situ by $(\text{Bu}_4\text{N})_3\text{HP}_2\text{O}_7$ in CH_3CN . Carbonate **32c** was not isolated, rather, *p*-hydroxymethyl PGPP **9c** was purified directly from the diphosphorylation reaction.

The other two hydroxymethyl PGPP derivatives **9a** and **9b** were obtained in quantitative yield by photolysis of the RP-HPLC purified carbonates **32a** and **32b** with Pyrex filtered UV light for 5–10 min in aqueous ammonium bicarbonate at 0°C . The advantage of photodeprotection is that the nitroso byproducts are separated from the pure analogue diphosphates **9a** and **9b** by CH_2Cl_2 extraction, avoiding additional chromatography (Scheme 4).

Analogue hydrophobicity depends on terminal aromatic moiety substituents

The lipophilicity of the anilino geranyl diphosphates **2a–ae** and phenoxygeranyl diphosphates **6a–ad** and **9a–c** is correlated with the apparent logP ($\log P^{app}$) of the parent alcohols (Table 2) and was determined from RP-HPLC capacity factors. LogP is the logarithm of the partition coefficient between water saturated octanol and octanol saturated water and is a useful metric of hydrophobicity and the ability of compounds to associate with membranes. The incorporation of aromatic rings and heteroatoms into the analogues decrease their hydrophobicity relative to farnesol.

FTase catalysis depends on isoprenoid size and shape, not hydrophobicity

The kinetic parameters $^{app}k_{cat}$, $^{app}K_m^{peptide}$ and apparent $k_{cat}/K_m^{peptide}$ were measured for transfer of each PGPP analogue to dns-GCVLS utilizing a continuous fluorescence assay (Table 2). Thirty one of the 33 PGPP analogues **6a–ad** and **9a–c** were detectably transferred to dns-GCVLS peptide by FTase (Table 2). The aryl substituents of 20 PGPP molecules were identical to previously reported AGPP analogues.^[32] In general, transfer kinetics and hydrophobicity of PGPP and AGPP analogues with identical aryl moieties were similar. The apparent logP of PGPP analogues varied within ± 1.3 units of the corresponding AGPP (Table 2) and apparent $k_{cat}/K_m^{peptide}$ were within a factor of ± 5.3 . However, there are a number of important differences in reactivity between the two different classes of FPP analogues. The *p*-Et-PGPP **6x**, *p*-*i*Pr-PGPP **6ab**, *m*-*i*Pr-PGPP **6aa**, *p*-Bn-PGPP **6ad** and *o*-I-PGPP **6s** analogues were efficient substrates, whereas corresponding AGPP analogues were not transferred to the dns-GCVLS peptide.^[32] Larger substituents in the transferable PGPP series may be productively accommodated in the FTase active site because the ether linkage is conformationally less restricted than the aniline linkage in the corresponding AGPP analogues. We found that the *meta*- and *para*-hydroxymethyl PGPP **9b** and **9c** were efficiently transferred by FTase while the *ortho*- isomer **9a** was not, further reinforcing the observation that reactivity depends on substituent position and size. Remarkably, the *para*-hydroxymethyl PGPP **9b** was almost as efficient a substrate as FPP, indicating that FTase activity is not necessarily decreased by hydrophilic lipid analogues.

FPP analogue transfer efficiency does not correlate with lipid hydrophobicity

The apparent $k_{cat}/K_m^{peptide}$, $^{app}K_m^{peptide}$ and $^{app}k_{cat}$ for the library of 54 transferable PGPP and AGPP analogues as well as GPP and FPP was plotted against apparent logP to determine if there was a simple relationship between FTase catalytic activity and the lipid shape, size and hydrophobicity (Figure 3).

Thirty nine different substituted aryl groups are represented in the library, where 15 substituents are identical in both the anilinogeranyl and phenoxygeranyl series, as well as eight unique AGPP and 16 unique PGPP structures. The hydrophobicity of the compounds in the library spanned six orders of magnitude and included molecules with both greater (*p*-*i*Pr-PGPP **6ab**, logP = 6.8) and substantially lower (Isox-GPP **8**, logP = 0.7) apparent logP than FPP (logP = 6.1). Surprisingly, we found no discernible relationship between apparent $k_{cat}/K_m^{peptide}$ and apparent logP of the transferable analogues. Similar plots of $^{app}k_{cat}$ vs. apparent logP and $^{app}K_m^{dns-GCVLS}$ vs. apparent logP also show no obvious relationship between the measured properties.

The pattern of analogue reactivity with dns-GCVLS leads to the surprising conclusion that isoprenoid transfer efficiency does not depend on lipid hydrophobicity. Rather, isoprenoid size and shape appear to be the most important lipid physical property for FTase catalyzed transfer to Ca_1a_2X peptides. This result is even more startling in light of the extensive contacts between the farnesyl hydrocarbon and the predominantly hydrophobic aromatic amino acid side chains in the enzyme active site revealed in X-ray crystal structures of the binary FTase•FPP and ternary FTase•FPP•CaaX and FTase•product complexes.^[26, 37–44] These observations are important because they indicate that the biological functions of the isoprenoid that depend on hydrophobic association with membranes and/or protein receptors are not critical for efficient transfer to Ca_1a_2X peptides by FTase. Furthermore, the results of these studies indicate that the role played by the farnesyl lipid in the FTase mechanism is primarily structural. Several data provide evidence to support these conclusions.

There are multiple points in the FTase mechanism where lipid binding is structurally important (Figure 1).^[26] Mutagenesis and computational studies suggest that the primary

source of free energy for FPP binding to FTase are electrostatic interactions between the negatively charged diphosphate group and the positively charged amino acid residues at the upper rim of the FTase active site.^[15, 45] The lipid binds to one wall of the FTase active site in an extended conformation in the E•FPP complex and forms a substantial part of the peptide binding site in the E•FPP•CaaX complex.^[40–41] Lipids such as GPP that are too small to adequately fill the farnesyl lipid binding site, as well as molecules that are substantially larger than FPP such as GGPP, are poor substrates for FTase.^[14–15, 46] Larger molecules physically interfere with the transfer reaction by occluding the peptide binding site.^[14, 18] The poor transfer kinetics for GPP (logP = 3.6) relative to FPP are not due to reduced lipophilicity of the geranyl group, as AGPP is almost identical in size to FPP, but has the same logP as GPP and is transferred to Ca₁a₂X peptides more efficiently than FPP.^[32] Additionally, a number of other analogues with a range of lipophilicities are transferred more efficiently to dns-GCVLS than FPP (Table 2), reinforcing the observation that the size and shape of the isoprenoid are critical determinants of transferability.^[32, 47] In particular, the divergent transfer efficiencies of the four most polar analogues, Isox-GPP **8** and *o*-, *m*-, *p*-hydroxymethyl PGPP **9a–c**, illustrate this point (Table 2).

The Ca₁a₂X peptide adopts a single extended conformation in the E•FPP•CaaX, E•Product and E•FPP•Product complexes.^[26] Notably, Ca₁a₂X peptides with a wide range of hydrophobicity and amino acid residues in the a₁, a₂ and X positions are productively accommodated in the active site in essentially the same conformation.^[26, 48] The third isoprene of the lipid diphosphate makes intimate contacts with the a₂ residue and the peptide backbone of the Ca₁a₂X peptide co-substrate in the E • FPP • CaaX, E-product and E•FPP•Product complexes.^[26] In contrast, contacts between the first and second isoprenes and FTase active site amino acid side chains are disrupted upon product formation and new interactions form between the lipid and the Ca₁a₂X peptide in the E•Product complex.^[26] It is clear that substantial changes in the structure, electronics and hydrophobicity of the terminal isoprene and its interactions with the Ca₁a₂X peptide do not interfere with achieving the transition state and product formation (Tables 1 & 2).^[32] The dissociation constant ($K_D^{peptide}$) for four Ca₁a₂X peptides with the FTase•FPP complex are very different from each other and are not correlated with $k_{cat}/K_m^{peptide}$.^[16] Furthermore, changes in the structure of the first and second isoprene can also yield transferable analogues.^[16, 49–52] However, there is no simple relationship between the structures of the lipid donor and peptide acceptor and their reactivity.

The thioether product is substantially more hydrophobic than either substrate and product release depends on binding of either a new lipid diphosphate or Ca₁a₂X peptide (Figure 1).^[40, 35] Product release stimulated by lipid diphosphate binding results in formation of the E•Product•FPP complex where two lipid moieties interact with the enzyme. The structure of this complex revealed by x-ray crystallographic analysis shows that the new FPP and alkylated peptide are in the active site while the farnesyl thioether is flipped out into an exit groove.^[26, 40, 53–54] Presumably, the association of the FPP and displacement of the alkylated lipid is driven by electrostatic interaction of the diphosphate moiety with the enzyme. Displacement of the alkylated peptide product by Ca₁a₂X peptide is consistent with the free energy of E•Product being higher than E•CaaX and the observation that farnesylation of competitive Ca₁a₂X peptides decreases their affinity for FTase.^[24] We have previously observed that AGPP may be less efficient than FPP at stimulating product release due to the decreased hydrophobicity of AGPP.^[32, 35] However, AGPP is transferred more efficiently to dns-GCVLS than is FPP, indicating that there may be greater flux through the peptide stimulated release pathway for AGPP compared with FPP at comparable isoprenoid concentrations. It is possible that analogues more hydrophilic than AGPP are even less efficient at stimulating product release from the E•Product complex due to their relatively stronger interactions with the bulk solvent water. However, the efficiency of peptide

stimulated release for some of the hydrophilic analogues (notably *p*-hydroxymethyl PGPP **9c** and *p*-CN-PGPP **6k**) must increase correspondingly, as their overall efficiency of transfer is comparable or significantly better than for FPP (Table 2).

The FTase active site stabilizes a membrane interface-like environment

The FTase active site is predominantly lined with tryptophan and tyrosine residues.^[26] Partition of tryptophan and tyrosine side chains into membrane interfaces is strongly favored while their partition into the membrane alkyl phase is disfavored.^[55] Zwitterionic membrane interfaces are about 15 Å thick and consist of a complex and thermally disordered mixture of water, charged lipid headgroups and methylenes from the edges of the hydrocarbon core.^[55] The highly favorable free energy for partition of both tryptophan and tyrosine side-chains into membrane interfaces suggests that the FTase active site lining stabilizes a membrane interface like volume. Similar to membrane interfaces, the FTase active site contains a large number of water molecules as well as a variety of charged groups. The Arg 202β, Glu 198β and Asp 200β side chains are at the bottom, and the highly polar diphosphate binding and Zn⁺² coordinating residues are at the upper rim of the active site. Small N-acyl peptides (1–6 residues) composed of non-polar or aromatic residues and charged C-termini are unstructured and partition almost exclusively into palmitoylcholine (POPC) membrane interfaces and are virtually insoluble in the membrane alkyl phase.^[55] The dns-GCVLS peptide as well as the C-termini of H-, K- and N-Ras are unstructured in solution and bind to FTase in an extended conformation.^[56] X-ray crystallographic analysis shows that Ca₁a₂X peptide substrate binding is mediated by interactions through ordered water molecules.^[39]

FPP and the transferable analogues are intrinsically flexible and adopt a number of interconverting conformations in solution.^[57] The conformational space accessible to the lipid chain in these molecules is significantly reduced upon binding to FTase.^[57] The loss of conformational entropy is proposed to be partially compensated for by contacts with the binding site as well as by displacement of waters hydrating the active site and lipid. Structural studies reveal that the terminal FPP isoprene is buried in a pocket formed from W102β, Y154β, Y205β, C254β, W303β and the dns-GCVLS leucine Ca₁a₂X a₂ side chain. Efficient transfer of the substantially less hydrophobic analogues implies that the free energy for lipid diphosphate association does not depend strongly on the lipid chain hydrophobicity. The FTase dissociation constant (K_D) for FPP and a series of four transferable FPP analogues with a range of hydrophobicities are similar to each other and are not correlated with k_{ca} or $K_m^{analogue}$ for transfer to dansyl-GCVLS.^[58] This is particularly important as farnesol preferentially partitions into alkyl phases relative to the aqueous phase (Table 2). The free energy change for moving amino acid side chains from water into a membrane interface is about 1/2 that of moving the same residue into the membrane alkyl phase.^[55] A membrane interface like active site would act to level both favorable and unfavorable changes in free energy for transfer of the substrates and products into and out of the FTase active site. Therefore, one function of the active site aromatic residues is to reduce the affinity of FTase for alkyl phases in order to facilitate release of the hydrophobic product once the diphosphate has been displaced. This is consistent with the observation that farnesol is a poor inhibitor of FTase. Interaction of the FPP lipid chain with the active site residues is important for orienting and tethering the charged diphosphate moiety in a conformation most conducive to binding and activation as a leaving group. Furthermore, the leveling effect allows the PGPP and AGPP series lipid chains to function as a structural anchor for the diphosphate leaving group despite their reduced hydrophobicity. Previously, Gibbs and co-workers developed a pharmacophore model for FPP analogues where hydrophobic elements were placed at the lipid C₃- and C₁₁-methyl groups to account for critical interactions observed in a variety of analogues.^[33, 51–52] Our observations that

efficiency of isoprenoid transfer does not depend on the lipid hydrophobicity, but does depend on the lipid moiety occupying an appropriate volume of the active site are consistent with this model.

Conclusion

These observations are consistent with an FTase active site that has evolved to either provide no net stabilization or which slightly destabilizes the association of alkyl groups (and phases) while stabilizing the binding of $\text{Ca}_1\text{a}_2\text{X}$ peptides with open hydrogen bonds. The conclusion that interactions between the FTase active site and alkyl phases are destabilized provides part of the explanation for why the substantially more hydrophobic farnesylated thioether product can be ejected from the active site by an incoming $\text{Ca}_1\text{a}_2\text{X}$ peptide. Loss of the diphosphate upon thioether formation removes much of the free energy driving binding of FPP to FTase, allowing displacement of the product by either a new lipid diphosphate or new $\text{Ca}_1\text{a}_2\text{X}$ peptide. These results also show that analogues with large changes in hydrophobicity engineered into the isoprenoid structure retain activity as FTase substrates, which may be important for the development of prenylated protein function inhibitors.

Experimental Section

All the reactions except for resin preparation were performed in PTFE tubes using a Quest 210 apparatus manufactured by Argonaut Technologies. All RP-HPLC was performed on an Agilent 1100 HPLC system equipped with a microplate autosampler, diode array and fluorescence detector. N-dansyl-GCVLS was purchased from Peptidogenics (San Jose, CA, USA). Spectrofluorometric analyses were performed in 96-well flat bottom, non-binding surface, black polystyrene plates (Corning, Excitation wavelength, 340 nm; emission wavelength 505 nm with a 10 nm cutoff) with a SpectraMax GEMINI XPS fluorescence well-plate reader. HPLC analysis of peptide reactions utilized a microsorb C18 column with 0.01% TFA in water (A) and 0.01% TFA CH_3CN (B) as the mobile phase as described [32]. Absorbance readings were determined using a Cary UV/Vis spectrophotometer. All assays were performed at minimum in triplicate where the average values are reported with a one standard of deviation error. Recombinant mammalian protein farnesyl transferase was a gift from Dr. Carol Fierke (University of Michigan). Reaction temperature refers to the external bath. All solvents and reagents were purchased from VWR (EM Science-Omnisolv high purity) and Aldrich respectively and used as received. Merrifield-Cl resin was purchased from Argonaut technologies. Synthetic products were purified by silica gel flash chromatography (EtOAc/hexane) unless otherwise noted. RP-HPLC purification of lipid diphosphates were carried out using a Varian Dynamax, 10 μm , 300 \AA , C-18 (10 mm \times 250 mm) column and eluted with a gradient mobile phase and flow rate of 4 mL/min: 90% of A and 10% of B linear increase to 100% of B and retained in the same ratio for two more minutes and brought back to 90% of A and 10% of B over 5 minutes and monitored at 254 nm & 210 nm. A is 25mM aqueous ammonium acetate, B is CH_3CN . ^1H NMR and ^{13}C NMR spectra of alcohols were obtained in CDCl_3 and ^1H and ^{31}P of diphosphates in D_2O with a Varian Inova spectrometer operating at 400 MHz (^1H), 100.6 MHz (^{13}C) and 161.8 MHz (^{31}P). Chemical shifts are reported in ppm from CDCl_3 internal peak at 7.27 ppm for ^1H and 77.4 ppm for ^{13}C ; D_2O (TSP, 0 ppm for ^1H ; H_3PO_4 as an external reference, 0 ppm for ^{31}P). ESI-MS were performed at the University of Kentucky Mass Spectra Facility. Positive and negative ion electrospray ionization (ESI) mass spectra were obtained on a Thermofinnigan LCQ with sample introduction by direct infusion. High resolution impact (EI) ionization mass spectra were recorded at 25eV on a JEOL JMS-700T MSstation (magnetic sector instrument) at a resolution of greater than 10000. Samples were introduced

via heatable direct probe inlet. Perfluorokerosine (pfk) was used to produce reference masses. Spectral data for all new molecules are reported in supplementary data.

Synthesis of Farnesyl diphosphate (FPP, **1**), Geranyldiphosphate (GPP, **11**) and Anilinogeranyl diphosphates (**2a–ae**)

FPP **1** and GPP **11** were prepared as described by Davisson et al.^[59] Anilinogeranyl analogues **2a–ae** were prepared on solid support or in solution as previously described by Subramanian and Chehade et al.^[20, 36]

2-((2E,6E)-8-chloro-3,7-dimethyl-octa-2,6-dienyloxy)-tetrahydro-pyran (13**)**—Chloride **12**^[60] (2 g, 1.06 mmol), dihydropyran (1.07 g, 1.27 mmol) and PPTS (50 mg) in dry methanol (10 mL) were stirred overnight at room temperature. The reaction mixture was concentrated, extracted into CH₂Cl₂, the organic phase was washed with sat. NaHCO₃, water, brine, dried (MgSO₄), filtered and concentrated. Chromatographic purification of the crude product gave chloride **13** in quantitative yield. The spectral data were consistent with previous reports.^[61]

2-((2E,6E)-3,7-Dimethyl-9-phenyl-nona-2,6-dienyloxy)-tetrahydro-pyran (14**)**—Benzyl magnesium chloride (3.68 mL, 1.0 M solution in Et₂O, 3.68 mmol) was added dropwise to a solution of **13** (1 g, 3.68 mmol) in Et₂O (20 mL) at 0 °C and stirred for 3 h. After allowing the reaction to warm to room temperature and stir overnight, it was diluted with sat. NH₄Cl (5 mL) and extracted with Et₂O (2X). The organic extracts were dried (MgSO₄), filtered and evaporated. Chromatographic purification of the oily residue gave ether **14** (994 mg, 83%).

(2E,6E)-3,7-Dimethyl-9-phenyl-nona-2,6-dien-1-ol (15**)**—Compound **14** (990 mg, 0.3 mmol) and PPTS (50 mg) were stirred in dry MeOH (5 mL) overnight. The reaction mixture was concentrated, extracted with ethyl acetate, washed with sat. NaHCO₃, brine, dried (MgSO₄), filtered and evaporated. Chromatographic purification of the residue gave alcohol **15** (670 mg, 91%).

(2E,6E)-3,7-Dimethyl-9-phenyl-nona-2,6-dien-1-diphosphate (3**)**—Ph₃PBr₂ (103 mg, 0.246 mmol) in CH₃CN (2 mL) was added dropwise to a cooled (0°C) solution of alcohol **15** (30 mg, 0.123 mmol) in CH₃CN (5 mL) and stirred for 2 h. ((n-Bu)₄N)₃HP₂O₇ (480 mg, 0.492 mmol) in CH₃CN (2 mL) was then added and the solution allowed to warm to room temperature over 30 min. The reaction mixture was concentrated and washed with Et₂O. The organic extracts were discarded and the residue suspended in 2 mL ion exchange buffer (25 mM NH₄HCO₃ in 2% (v/v) *i*-PrOH/water). The resultant white solution was loaded onto a preequilibrated 4×30 cm column of Dowex AG 50W-X8 (100–200 mesh) cation-exchange resin (NH₄⁺ form). The flask was washed with buffer (2 × 2 mL) and loaded onto the column before eluting with 100 mL of ion exchange buffer. The eluent was lyophilized to yield a white solid. This solid was dissolved in 25 mM solution of NH₄HCO₃ buffer (4 mL), purified by RP-HPLC (retention time about 7 min.) and lyophilized to give **3** (18 mg, 32%) as a white powder.

General procedure for synthesis of alcohols **19a–c**

Compound **17** (either **17a–c**: 0.45 mmol) in THF (2 mL) was added dropwise to a stirred suspension of NaH (182 mg, 0.45 mmol) in THF (5 mL) at 0°C and allowed to stir for 1 h. Bromide **16** (1.25 g, 0.45 mmol) in THF (5 mL) was added and stirred at 0°C for 1 h. After the reaction was allowed to warm to room temperature and stirred overnight, then diluted by slow addition of water, concentrated and extracted with CH₂Cl₂. The organics were washed with water, brine, dried (MgSO₄), filtered and concentrated. The residue was dissolved in

MeOH (5 mL) and stirred at room temperature overnight with K_2CO_3 (1.9 g, 1.35 mmol). The reaction mixture was concentrated, extracted with ethyl acetate. The organics were washed with water, brine and concentrated *in vacuo*. Chromatography of the residue gave **19a–c** (0.988 g of **19a**: 83%; 0.886 g of **19b**: 75%; 1.16 g of **19c**: 73%).

General procedure for synthesis of diphosphates **4**, **5** and **7**

Alcohol **19** (either **19a–c**, 30 mg each) was stirred with Ph_3PCl_2 (2 equiv.) in dry CH_3CN (3 mL) at $0^\circ C$ and allowed to warm to room temperature over 1h and stirred at the same temperature for 10 h. $((n-Bu)_4N)_3HP_2O_7$ (480 mg, 0.492 mmol) in CH_3CN (2 mL) was then added and stirred for 3 h at room temperature. The lipid diphosphate was isolated as described above for compound **3** (14 mg of **4**: 26%, 21 mg of **5**: 38%, 23 mg of **7**: 47%).

Resin-bound alcohol 21—Resin **20** (11.62 g, 1.87 mmol/g, 21.7mmol) was agitated with DCE/EtOH (200 mL, 1:1) for 20 min followed by addition of $NaBH_4$ (1.10 g, 30 mmol) in small portions. The resultant mixture was agitated for 3 h at room temperature and then heated to $50^\circ C$ for 12 h. The reaction mixture was cooled to room temperature and filtered. The resin was thoroughly washed with 1:1 THF/ H_2O (3X), 1:1 MeOH/ H_2O (3X), THF (3X), 1:1 MeOH/ CH_2Cl_2 (3X) and CH_2Cl_2 and dried (11.68 gm).

General Procedure for resin cleavage

Resin **21** (500 mg, 0.935 mmol) in 10 mL of DCE/MeOH (1:1 v/v) and PPTS (50 mg, 0.199 mmol) was heated at reflux for 12 h. The cooled resin was filtered, washed with CH_2Cl_2 (3X) and the combined filtrate was concentrated. The residue was extracted with ethyl acetate, washed with sat. $NaHCO_3$, water, dried ($MgSO_4$), filtered and concentrated. Chromatographic purification of the crude product gave diol **22** (128 mg, 81%). The spectral data were consistent with previous reports.^[62]

General Procedure for Alcohols **24a–ad** (Mitsunobu reaction)

Four equivalent of DEAD (0.217 mL, 0.608 mmol, 40% solution in toluene) was added to a suspension of resin **21** (100 mg, 1.52 mmol/g, 0.152 mmol), Ph_3P (159 mg, 0.608 mmol) and appropriate phenol (4 equiv.) in DCE (4 mL) and agitated overnight. Product resin **23a–ad** was washed with CH_2Cl_2 (5X) and THF (5X) and dried under vacuum. The alcohols **24a–ad** were cleaved from the dried resin as for **22** above.

General Procedure for the Synthesis of Phenoxygeranyldiphosphates (**6a–ad**)

Ph_3PBr_2 (71 mg, 0.168 mmol) was added to resin **23a–ad** (1.352 mmol/g) pre-swollen in dry CH_2Cl_2 and agitated for 3 h under N_2 . $((n-Bu)_4N)_3HP_2O_7$ (760 mg, 0.775 mmol) in dry CH_3CN (3 mL) was then added and agitated for 3 h at room temperature. The resultant heterogeneous mixture was filtered and the solid washed twice with dry CH_3CN . The lipid diphosphate **6a–ad** was isolated from the combined filtrate as described above for compound **3**.

General Procedure for THP ethers **27a–c**

DEAD (1.9 mL, 40% in toluene, 4.25 mmol) was added dropwise to a stirred solution of **25** (900 mg, 3.5 mmol), phenol **26** (518 mg for **26b** and **26c**, 646 mg in case of **26a**, 4.25 mmol), Ph_3P (1.11 g 4.25 mmol) in THF (10 mL) at $0^\circ C$ and stirred for 1 h. After allowing the reaction to warm to room temperature and stir overnight, it was diluted with sat. $NaHCO_3$, concentrated, and extracted with CH_2Cl_2 (2X). The organic extracts were dried ($MgSO_4$), filtered and concentrated. Chromatographic purification of the oily residue gave **27a–c** (912 mg of **27a** : 66%, 1.05 g of **27b** : 83%, 702 mg of **27c** : 55%).

General Procedure for hydroxymethyl-phenoxygeranyl-THP ethers **28a–c**

NaBH₄ (104 mg, 2.6 mmol) was added to ether **27** (1.3 mmol of **27a–c**) in EtOH (10 mL) at 0°C and stirred for 3 h. The mixture was diluted with water and extracted with CH₂Cl₂ (2X). The organic extracts were dried (MgSO₄), filtered and evaporated. Chromatographic purification of the oily residue gave **28a–c** in quantitative yield.

General Procedure for diols **29a–c**

Ether **28** (**28a–c**, 100 mg, 0.27 mmol) was stirred with PPTS (20 mg) in dry CH₃OH (3 mL) overnight at room temperature. The solvent was evaporated and the residue extracted with ethyl acetate (2 × 20 mL). The organic extracts were washed with sat. NaHCO₃, brine, dried (MgSO₄), filtered and evaporated. Chromatographic purification of the oily residue gave **29a–c** in quantitative yield.

General Procedure for carbonates **30a, 30b and 30c**

[**Caution!** α -methyl-*o*-nitrobenzyl chloroformate^[63] was prepared in-situ using the highly toxic phosgene.^[64] The reaction and subsequent work up must be carried out in an efficient fume hood!] Ether **28** (**28a–c**, 150 mg, 0.41 mmoles) in 1:3 pyridine/CH₂Cl₂ (4 mL) was added dropwise to a solution of α -methyl-*o*-nitrobenzyl chloroformate (165 mg, 0.41 mmoles) in dry CH₂Cl₂ (3 mL) at 0°C. The reaction was allowed to warm to room temperature and stirred for 24 h. The solvent was removed under vacuum and the residue was dissolved in CH₂Cl₂ (20 mL), washed with 1M NaHSO₃ (2X), brine, dried (MgSO₄), filtered and evaporated. Chromatographic purification of the oily residue gave 158mg of **30a**: 69%, 174 mg of **30b**: 76%, 168mg of **30c**: 73%).

General Procedure for compounds **31a–c**

Compounds **31a–c** were prepared from ethers **30a–c** (100 mg, 0.18 mmol) by the same method as **29a–c** above (Yield, 72mg of **31a**: 85%, 69mg of **31b**: 82%, 70mg of **31c**: 83%).

General Procedure for hydroxymethyl diphosphates **32a–c**

Ph₃PBr₂ (45 mg, 0.106 mmol) in CH₃CN (3 mL) was added dropwise to a cooled (0°C) solution of alcohol **31** (**31a–c**, 50 mg, 0.106 mmol) in CH₃CN (2 mL) and stirred for 3 h. ((n-Bu)₄N)₃HP₂O₇ (417 mg, 0.424 mmol) in CH₃CN (2 mL) was then added and the solution allowed to warm to room temperature over 1 h. The reaction mixture was worked up and diphosphates **32a–b** isolated as for **3** above (31 mg of **32a**: 31%, 28 mg of **32b**: 39%, 18 mg of **9c**: 35%). The compound **32c** was unstable and obtained as **9c**.

Preparation of compounds **9a and 9b**

Compound **31a** or **31b** (10 mg) in 25 mM solution of NH₄HCO₃ (1 mL) was irradiated with pyrex filtered UV light for 5 min at 0°C in a Rayonet device. The yellow solution was extracted with CH₂Cl₂, the organics discarded and aqueous layer lyophilized to obtain **9a/9b** in quantitative yield.

Steady-state peptide kinetics—The kinetic constants $appk_{cat}$, $appK_m^{peptide}$ and apparent $k_{cat}/K_m^{peptide}$ for transfer of isoprenoids **1**, **6a–6ad** by FTase to peptide were determined using a continuous spectrofluorometric assay originally developed by Pompliano et al. [65] and modified for a 96-well plate format as described.^[32] Analogue transfer to peptide was analyzed using reverse phase high performance liquid chromatography (RP-HPLC) as described.^[32]

LogP Determination—The apparent logP values for the corresponding alcohols **24a–ad** were estimated from the capacity factors (k') using reverse phase high performance liquid chromatography (RP-HPLC).^[12]

Acknowledgments

We thank Dr. Carol Fierke, Heather Hartman, Katherine Hicks and Jennifer Pickett, University of Michigan, for the gift of mammalian protein farnesyl transferase and Dr. Trevor Creamer, University of Kentucky, for helpful discussions.

Abbreviations

| | |
|--------------------|---|
| FTase | protein farnesyltransferase |
| FPP | farnesyl diphosphate |
| GGTase-I | protein geranylgeranyltransferase type 1 |
| GPP | geranyl diphosphate |
| GGPP | geranylgeranyl diphosphate |
| FTI | protein farnesyltransferase inhibitor |
| PFI | prenyl function inhibitor |
| CaaX | tetrapeptide sequence cysteine-aliphatic amino acid-aliphatic amino acid-X (serine, glutamine, or methionine for FTase) |
| dns | dansylated |
| RP-HPLC | reverse-phase high-performance liquid chromatography |
| H-Ras | Harvey-Ras |
| K-Ras | Kirsten-Ras |
| N-Ras | neuronal-Ras |
| AGPP | 8-anilinogeranyl diphosphate |
| PGPP | 8-phenoxygeranyl diphosphate |
| $appk_{cat}$ | apparent turnover number |
| $appK_m^{peptide}$ | apparent Michaelis-Menten constant for peptide |

References

1. Basso AD, Kirschmeier P, Bishop WR. *J Lipid Res.* 2006; 47:15–31. [PubMed: 16278491]
2. Gotlib J. *Curr Hematol Rep.* 2005; 4:77–84. [PubMed: 15610664]
3. Isobe T, Herbst RS, Onn A. *Semin Oncol.* 2005; 32:315–328. [PubMed: 15988686]
4. Khuri FR. *Clin Lung Cancer.* 2003; 5(Suppl 1):S36–40. [PubMed: 14641993]
5. Mitsch A, Bergemann S, Gust R, Sattler I, Schlitzer M. *Arch Pharm (Weinheim).* 2003; 336:242–250. [PubMed: 12916059]
6. Doll RJ, Kirschmeier P, Bishop WR. *Curr Opin Drug Discov Devel.* 2004; 7:478–486.
7. Woo JT, Nakagawa H, Krecic AM, Nagai K, Hamilton AD, Sebti SM, Stern PH. *Biochem Pharmacol.* 2005; 69:87–95. [PubMed: 15588717]
8. James GL, Brown MS, Goldstein JL. *Methods Enzymol.* 1995; 255:38–46. [PubMed: 8524124]
9. Cox AD, Der CJ. *Biochim Biophys Acta.* 1997; 1333:F51–71. [PubMed: 9294018]
10. Sebti SM. *Oncologist.* 2003; 8:30–38. [PubMed: 14671226]

11. Gibbs BS, Zahn TJ, Mu Y, Sebolt-Leopold JS, Gibbs RA. *J Med Chem.* 1999; 42:3800–3808. [PubMed: 10508429]
12. Roberts MJ, Troutman JM, Chehade KA, Cha HC, Kao JP, Huang X, Zhan CG, Peterson YK, Subramanian T, Kamalakkannan S, Andres DA, Spielmann HP. *Biochemistry.* 2006; 45:15862–15872. [PubMed: 17176109]
13. Dudler T, Gelb MH. *Biochemistry.* 1997; 36:12434–12441. [PubMed: 9376347]
14. Micali E, Chehade KA, Isaacs RJ, Andres DA, Spielmann HP. *Biochemistry.* 2001; 40:12254–12265. [PubMed: 11591144]
15. Chehade KA, Kiegiel K, Isaacs RJ, Pickett JS, Bowers KE, Fierke CA, Andres DA, Spielmann HP. *J Am Chem Soc.* 2002; 124:8206–8219. [PubMed: 12105898]
16. Reigard SA, Zahn TJ, Haworth KB, Hicks KA, Fierke CA, Gibbs RA. *Biochemistry.* 2005; 44:11214–11223. [PubMed: 16101305]
17. Kale TA, Hsieh SA, Rose MW, Distefano MD. *Curr Top Med Chem.* 2003; 3:1043–1074. [PubMed: 12769708]
18. Turek-Etienne TC, Strickland CL, Distefano MD. *Biochemistry.* 2003; 42:3716–3724. [PubMed: 12667062]
19. Lepre CA, Peng J, Fejzo J, Abdul-Manan N, Pocas J, Jacobs M, Xie X, Moore JM. *Comb Chem High Throughput Screen.* 2002; 5:583–590. [PubMed: 12470255]
20. Chehade KA, Andres DA, Morimoto H, Spielmann HP. *J Org Chem.* 2000; 65:3027–3033. [PubMed: 10814193]
21. Gaon I, Turek TC, Weller VA, Edelstein RL, Singh SK, Distefano MD. *J Org Chem.* 1996; 61:7738–7745. [PubMed: 11667728]
22. Rawat DS, Gibbs RA. *Org Lett.* 2002; 4:3027–3030. [PubMed: 12201708]
23. Stremler KE, Poulter CD. *J Am Chem Soc.* 1987; 109:5542–5544.
24. Moores SL, Schaber MD, Mosser SD, Rands E, O'Hara MB, Garsky VM, Marshall MS, Pompliano DL, Gibbs JB. *J Biol Chem.* 1991; 266:14603–14610. [PubMed: 1860864]
25. Furfine ES, Leban JJ, Landavazo A, Moomaw JF, Casey PJ. *Biochemistry.* 1995; 34:6857–6862. [PubMed: 7756316]
26. Long SB, Casey PJ, Beese LS. *Nature.* 2002; 415:645–650. [PubMed: 12374986]
27. Dolence JM, Poulter CD. *Proc Natl Acad Sci U S A.* 1995; 92:5008–5011. [PubMed: 7761439]
28. Huang C, Hightower KE, Fierke CA. *Biochemistry.* 2000; 39:2593–2602. [PubMed: 10704208]
29. Pompliano DL, Rands E, Schaber MD, Mosser SD, Anthony NJ, Gibbs JB. *Biochemistry.* 1992; 31:3800–3807. [PubMed: 1567835]
30. Troutman JM, Roberts MJ, Andres DA, Spielmann HP. *Bioconjug Chem.* 2005; 16:1209–1217. [PubMed: 16173800]
31. Coffinier C, Hudon SE, Lee R, Farber EA, Nobumori C, Miner JH, Andres DA, Spielmann HP, Hrycyna CA, Fong LG, Young SG. *J Biol Chem.* 2008; 283:9797–9804. [PubMed: 18230615]
32. Troutman JM, Subramanian T, Andres DA, Spielmann HP. *Biochemistry.* 2007; 46:11310–11321. [PubMed: 17854205]
33. Henriksen BS, Zahn TJ, Evanseck JD, Firestine SM, Gibbs RA. *J Chem Inf Model.* 2005; 45:1047–1052. [PubMed: 16045300]
34. Spencer TA, Onofrey TJ, Cann RO, Russel JS, Lee LE, Blanchard DE, Castro A, Gu P, Jiang GJ, Shechter I. *J Org Chem.* 1999; 64:807–818. [PubMed: 11674151]
35. Troutman JM, Andres DA, Spielmann HP. *Biochemistry.* 2007; 46:11299–11309. [PubMed: 17877368]
36. Subramanian T, Wang Z, Troutman JM, Andres DA, Spielmann HP. *Org Lett.* 2005; 7:2109–2112. [PubMed: 15901146]
37. Long SB, Hancock PJ, Kral AM, Hellinga HW, Beese LS. *Proc Natl Acad Sci U S A.* 2001; 98:12948–12953. [PubMed: 11687658]
38. Long SB, Casey PJ, Beese LS. *Structure.* 2000; 8:209–222. [PubMed: 10673434]
39. Strickland CL, Windsor WT, Syto R, Wang L, Bond R, Wu Z, Schwartz J, Le HV, Beese LS, Weber PC. *Biochemistry.* 1998; 37:16601–16611. [PubMed: 9843427]

40. Long SB, Casey PJ, Beese LS. *Biochemistry*. 1998; 37:9612–9618. [PubMed: 9657673]
41. Dunten P, Kammlott U, Crowther R, Weber D, Palermo R, Birktoft J. *Biochemistry*. 1998; 37:7907–7912. [PubMed: 9609683]
42. Park HW, Boduluri SR, Moomaw JF, Casey PJ, Beese LS. *Science*. 1997; 275:1800–1804. [PubMed: 9065406]
43. Hightower KE, De S, Weinbaum C, Spence RA, Casey PJ. *Biochem J*. 2001; 360:625–631. [PubMed: 11736652]
44. Wu Z, Demma M, Strickland CL, Radisky ES, Poulter CD, Le HV, Windsor WT. *Biochemistry*. 1999; 38:11239–11249. [PubMed: 10471273]
45. Cui G, Wang B, Merz KM Jr. *Biochemistry*. 2005; 44:16513–16523. [PubMed: 16342942]
46. Reiss Y, Seabra MC, Armstrong SA, Slaughter CA, Goldstein JL, Brown MS. *J Biol Chem*. 1991; 266:10672–10677. [PubMed: 2037606]
47. Turek TC, Gaon I, Distefano MD, Strickland CL. *J Org Chem*. 2001; 66:3253–3264. [PubMed: 11348105]
48. Krzyziak AJ, Scott SA, Hicks KA, Fierke CA, Gibbs RA. *Bioorg Med Chem Lett*. 2007; 17:5548–5551. [PubMed: 17804232]
49. Mu Y, Eubanks LM, Poulter CD, Gibbs RA. *Bioorg Med Chem*. 2002; 10:1207–1219. [PubMed: 11886785]
50. Zahn TJ, Weinbaum C, Gibbs RA. *Bioorg Med Chem Lett*. 2000; 10:1763–1766. [PubMed: 10937743]
51. Shao Y, Eummer JT, Gibbs RA. *Org Lett*. 1999; 1:627–630. [PubMed: 10823190]
52. Mu Y, Gibbs RA, Eubanks LM, Poulter CD. *J Org Chem*. 1996; 61:8010–8015. [PubMed: 11667783]
53. Wlodarczyk N, Gilleron P, Millet R, Houssin R, Goossens JF, Lemoine A, Pommery N, Wei MX, Henichart JP. *Oncol Res*. 2005; 16:107–118. [PubMed: 16925112]
54. Reid TS, Terry KL, Casey PJ, Beese LS. *J Mol Biol*. 2004; 343:417–433. [PubMed: 15451670]
55. Wimley WC, White SH. *Nat Struct Biol*. 1996; 3:842–848. [PubMed: 8836100]
56. Thapar R, Williams JG, Campbell SL. *J Mol Biol*. 2004; 343:1391–1408. [PubMed: 15491620]
57. Cui G, Merz KM Jr. *Biochemistry*. 2007; 46:12375–12381. [PubMed: 17918965]
58. Nguyen UTT, Crammer J, Gomis J, Reents R, Gutierrez-Rodriguez M, Goody RS, Alexandrov K, Waldmann H. *ChemBiochem*. 2007; 8:408–423. [PubMed: 17279592]
59. Davisson VJ, Woodside AB, Neal TR, Stremler KE, Muehlbacher M, Poulter CD. *J Org Chem*. 1986; 51:4768–4779.
60. Marshall JA, Lebreton J. *J Org Chem*. 1988; 53:4108–4112.
61. Nishitani K, Konomi T, Mimaki Y, Tsunoda T, Yamakawa K. *Heterocycles*. 1993; 36:1957–1960.
62. Williams JR, Lin C, Chodosh DF. *J Org Chem*. 1985; 50:5815–5822.
63. Hasan A, Stengele KP, Giegrich H, Cornwell P, Isham KR, Sachleben RA, Pfeleiderer W, Foote RS. *Tetrahedron*. 1997; 53:4247–4264.
64. Li S, Bowerman D, Marthandan N, Klyza S, Luebke KJ, Garner HR, Kodadek T. *J Am Chem Soc*. 2004; 126:4088–4089. [PubMed: 15053581]
65. Pompliano DL, Gomez RP, Anthony NJ. *J Am Chem Soc*. 1992; 114:7945–7946.

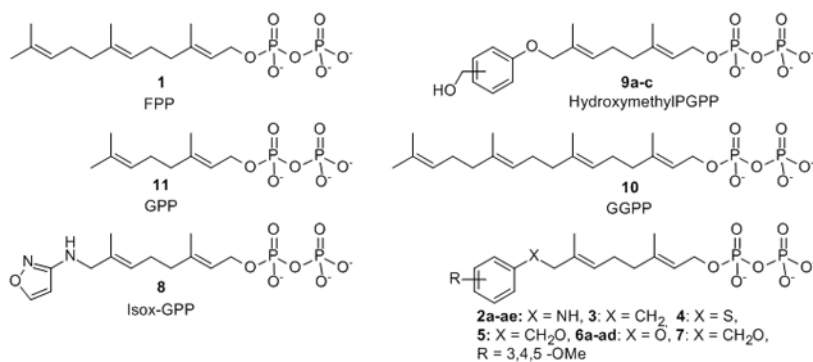
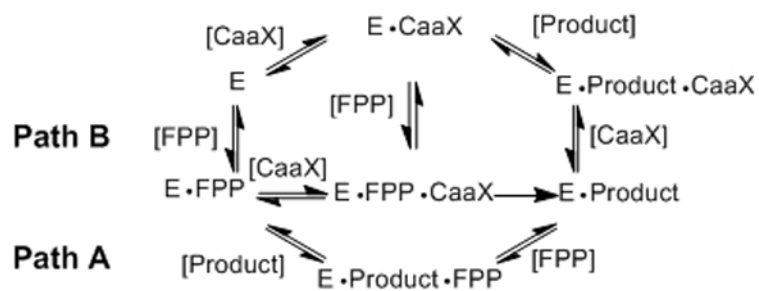


Figure 1.
FPP, GPP, GGPP and FPP analogues.

**Figure 2.**

FTase reaction mechanism showing two pathways. **Path A** represents FPP stimulated product release, and **Path B** represents peptide stimulated product release. E is the FTase enzyme, E•FPP is the FTase•FPP complex, E•FPP•CaaX is the FTase•FPP•CaaX peptide complex, E•Product is the FTase bound product complex, E•Product•FPP is the FTase bound to both FPP and the reaction product, E•CaaX is the peptide bound FTase inhibitory complex, and E•Product•CaaX is the peptide bound enzyme product complex.

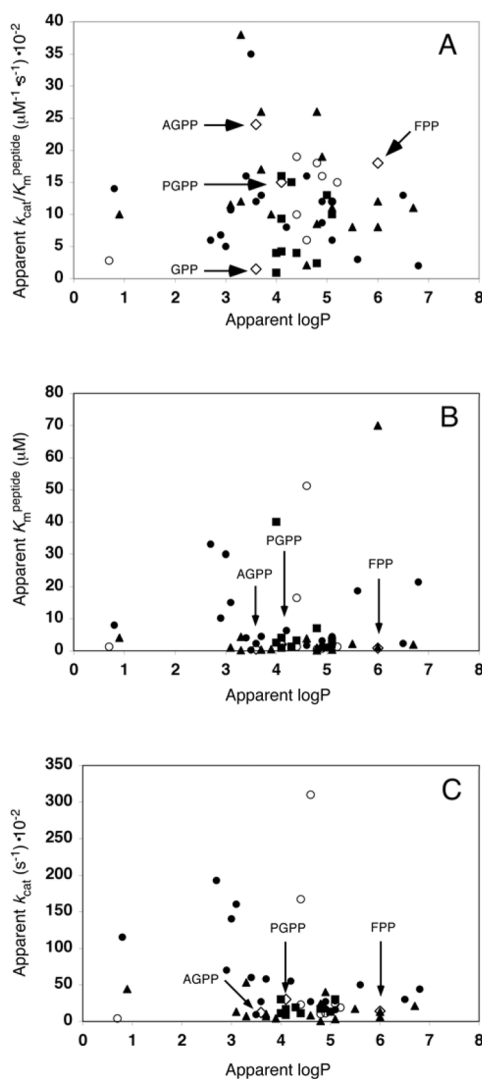
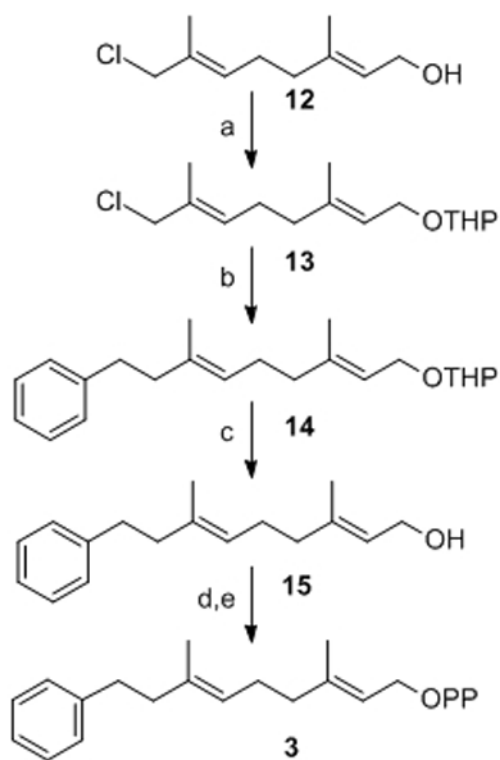
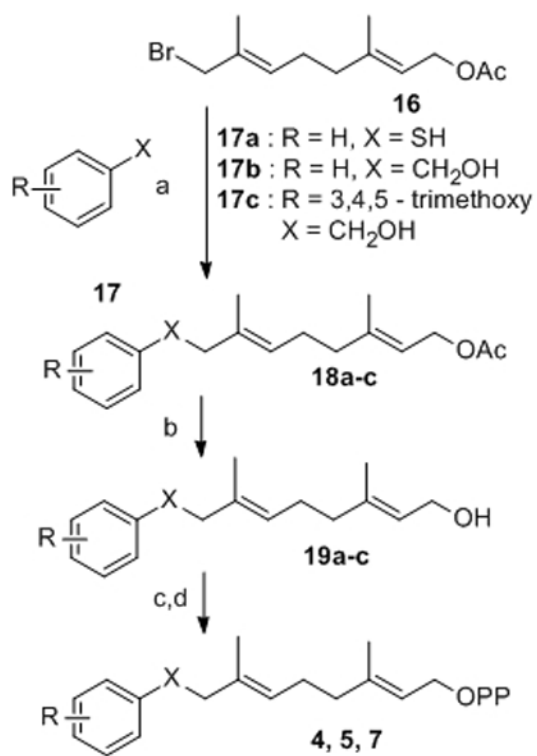


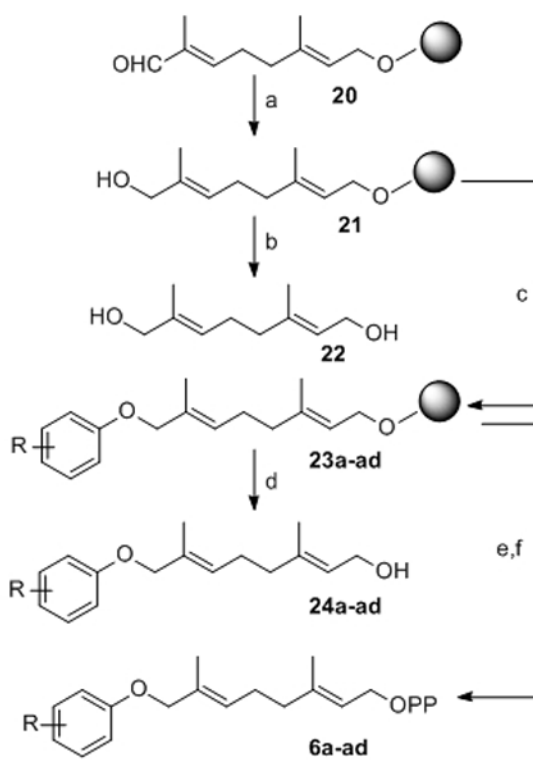
Figure 3. Plot of apparent logP vs apparent k_{cat}/K_m peptide for FPP, GPP and 54 transferable AGPP and PGPP analogues with dns-GCVLS. There are 39 different aryl structures present in the analogue library, where 16 are unique to the PG series, 8 unique to the AG series and 15 represented in both. The open diamonds \blacklozenge are FPP, GPP, AGPP and PGPP as indicated, the solid squares \blacksquare are ortho-, solid triangles \blacktriangle are meta-, solid circles \bullet are para- substituted analogues and the open circles \circ are Isox-GPP and multi-substituted PG analogues. The underlying data is from table 2.

**Scheme 1.**

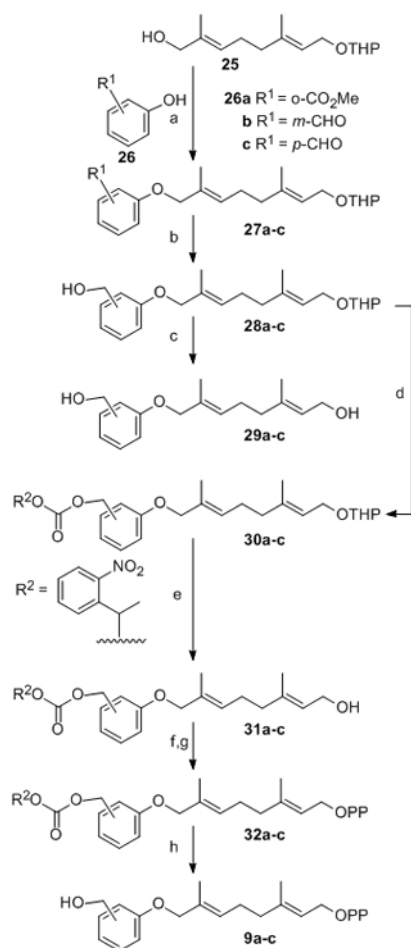
Synthesis of (2E,6E)-3,7-Dimethyl-9-phenyl-nona-2,6-dien-1-diphosphate: a) PPTS, DHP, DCE; b) PhCH₂MgCl, Et₂O, 0°C; c) PPTS, MeOH; d) Ph₃PBr₂, CH₃CN; e) (Bu₄N)₃HP₂O₇, CH₃CN.

**Scheme 2.**

Synthesis of diphosphates **4, 5, 7**: a) NaH, THF; b) K₂CO₃, MeOH/H₂O; c) Ph₃PBr₂, CH₃CN; d) (Bu₄N)₃HP₂O₇, CH₃CN.

**Scheme 3.**

Synthesis of phenoxygeranyl diphosphates **6a–6ad**: a) NaBH_4 , DCE/EtOH; b) PPTS, MeOH/DCE, reflux; c) Ph_3P , DEAD, Phenols, DCE; d) PPTS, MeOH/DCE, reflux; e) Ph_3PBr_2 , CH_2Cl_2 ; f) $(\text{Bu}_4\text{N})_3\text{HP}_2\text{O}_7$, CH_3CN

**Scheme 4.**

Synthesis of Hydroxymethylphenoxygeranyl diphosphate: a) DEAD, Ph₃P, THF; b) NaBH₄, EtOH; c) PPTS, MeOH; d) α -methyl-*o*-nitrobenzyl chloroformate, 3-pyridine/CH₂Cl₂; e) PPTS, MeOH; f) Ph₃PBr₂, CH₃CN; g) (Bu₄N)₃HP₂O₇, CH₃CN; h) NH₄HCO₃/H₂O, h ν , 0°C.

Table 1
Steady-state kinetic properties of FPP diphosphate analogues for reaction with dns-GCVLS

| R-group and position on ring [a] | Compound number | Apparent logP [b] | apparent k_{cat} [c] (s^{-1}) $\cdot 10^{-2}$ | apparent $K_m^{dns-GCVLS}$ [c] (μM) | apparent $k_{cat}/K_m^{dns-GCVLS}$ [c] ($\mu M^{-1}\cdot s^{-1}$) $\cdot 10^{-2}$ |
|---------------------------------------|-----------------|-------------------|---|--|---|
| NH | 2a | 3.6 | 10 \pm 3 | 0.4 \pm 0 | 20 \pm 4 |
| CH ₂ | 3 | 4.8 | 40 \pm 2 | 3.8 \pm 0.3 | 11 \pm 8 |
| S | 4 | 4.8 | 17 \pm 0.5 | 2.0 \pm 0.1 | 8 \pm 2 |
| CH ₂ O | 5 | 4.0 | 17 \pm 0.3 | 1 \pm 0.4 | 17 \pm 10 |
| O | 6a | 4.1 | 30 \pm 2 | 2.0 \pm 0.2 | 16 \pm 8 |
| CH ₂ O, X=3,4,5-Trimethoxy | 7 | 3.2 | Nde [d] | Nde [d] | Nde [d] |

[a] The analogues are listed in order of increasing substituent surface area.

[b] LogP measurements of the corresponding alcohol.

[c] $app k_{cat}$, $app K_m^{peptide}$ and apparent $k_{cat}/K_m^{peptide}$ were determined using a Michaelis-Menton analysis as described. [32]

[d] Nde indicates not determined.

Table 2
Hydrophobicity and steady-state kinetic properties of isoprenoids for reaction with dns-GCVLS

| R-group and position on ring [a] | Compound number | Apparent logP [b] | apparent $k_{cat}[c] (s^{-1}) \cdot 10^{-2}$ | apparent $K_m^{dns-GCVLS}[c] (\mu M)$ | apparent $k_{cat}/K_m^{dns-GCVLS}[c] (\mu M^{-1} s^{-1}) \cdot 10^{-2}$ |
|----------------------------------|-----------------|-------------------|--|---------------------------------------|---|
| GPP | 11 | 3.6 | 0.4 ± 0.1 | 27 ± 9 | 1.5 ± 0.7 |
| Isox-GPP | 8 | 0.7 | 4 ± 1 | 1.3 ± 0.4 | 2.8 ± 0.2 |
| FPP | 1 | 6.1 | 14 ± 2 | 0.8 ± 0.1 | 18 ± 3 |
| H | 6a | 4.1 | 30 ± 2 | 2.0 ± 0.2 | 15 ± 2 |
| H | 2a | 3.6 | 12 ± 2 [d] | 0.5 ± 0.1 [d] | 24 ± 6 [d] |
| o-F | 6b | 4.3 | 19 ± 1 | 1.3 ± 0.1 | 15 ± 3 |
| m-F | 6c | 4.8 | 0.4 ± 0.04 | 0.1 ± 0.015 | 8.5 ± 1.6 |
| p-F | 6d | 3.7 | 58 ± 5 | 4.5 ± 0.5 | 13 ± 3 |
| o-F | 2b | 4.1 | 15 ± 3 [d] | 0.9 ± 0.2 [d] | 16 ± 1 [d] |
| m-F | 2c | 3.7 | 10 ± 1 [d] | 0.34 ± 0.08 [d] | 26 ± 3 [d] |
| p-F | 2d | 3.5 | 9.5 ± 0.4 [d] | 0.26 ± 0.04 [d] | 35 ± 4 [d] |
| 2,6-di-F | 6e | 4.4 | 167 ± 3 | 16.5 ± 0.6 | 10 ± 2 |
| 3,4-di-F | 6f | 4.9 | 11 ± 0.4 | 0.7 ± 0.05 | 16 ± 4 |
| 2,3-di-F | 6g | 4.4 | 23 ± 0.5 | 1.3 ± 0.7 | 19 ± 1 |
| 3,5-di-F | 6h | 4.8 | 10 ± 0.2 | 0.5 ± 0.02 | 18 ± 2 |
| 2,3,5,6-tetra-F | 6i | 4.6 | 310 ± 2 | 51.2 ± 3.9 | 6 ± 1 |
| m-CN | 6j | 3.9 | 4 ± 0.1 | 0.42 ± 0.02 | 10 ± 2 |
| p-CN | 6k | 2.7 | 193 ± 9 | 33 ± 2.3 | 6 ± 2 |
| m-CN | 2h | 3.1 | 13 ± 1 [d] | 1.0 ± 0.1 [d] | 11.5 ± 0.3 [d] |
| p-CN | 2i | 2.9 | 70 ± 3 [d] | 10.2 ± 0.6 [d] | 6.8 ± 0.1 [d] |
| p-NO ₂ | 6l | 4.2 | 55 ± 2 | 6.3 ± 0.4 | 8 ± 1 |
| p-NO ₂ | 2j | 3.1 | 160 ± 20 [d] | 15 ± 2 [d] | 10.7 ± 0.2 [d] |
| o-Br | 6m | 5.1 | 30 ± 3 | 3.1 ± 0.34 | 10 ± 1 |
| m-Br | 6n | 6.0 | 6 ± 0.4 | 70 ± 0.1 | 8 ± 2 |
| p-Br | 6o | 5.6 | 50 ± 1 | 18.7 ± 0.8 | 3 ± 1 |
| o-Br | 2k | 5 | 13 ± 1 [d] | 1.0 ± 0.2 [d] | 13 ± 3 [d] |
| p-Br | 2l | 4.6 | 27 ± 8 [d] | 1.7 ± 0.5 [d] | 16 ± 2 [d] |

| R-group and position on ring [a] | Compound number | Apparent logP [b] | apparent $k_{cat} [c] (s^{-1}) \times 10^{-2}$ | apparent $K_m^{dms-GCVLS} [c] (\mu M)$ | apparent $k_{cat}/K_m^{dms-GCVLS} [c] (\mu M^{-1} s^{-1}) \times 10^{-2}$ |
|----------------------------------|-----------------|-------------------|--|--|---|
| o-CH ₃ | 2m | 4.1 | 16.6 ± 0.9 [d] | 4.0 ± 0.4 [d] | 4.2 ± 0.5 [d] |
| m-CH ₃ | 2n | 3.3 | 6.9 ± 0.5 [d] | 0.17 ± 0.06 [d] | 38 ± 8 [d] |
| p-CH ₃ | 2o | 3.4 | 60 ± 20 [d] | 4 ± 1 [d] | 16 ± 1 [d] |
| o-CF ₃ | 2p | 4 | 30 ± 10 [d] | >10 [d] | 0.9 ± 0.1 [d] |
| m-CF ₃ | 6p | 6.0 | 13 ± 0.5 | 1.1 ± 0.1 | 12 ± 2 |
| 3,5-di-Cl | 6q | 5.2 | 19 ± 0.7 | 1.3 ± 0.1 | 15 ± 2 |
| 3,4-di-Cl | 6r | 5.1 | 24 ± 1 | 2.1 ± 0.13 | 12 ± 2 |
| o-I | 6s | 4.4 | 11 ± 0.5 | 3.2 ± 0.20 | 4 ± 1 |
| m-I | 6t | 3.7 | 7 ± 0.2 | 0.4 ± 0.02 | 17 ± 2 |
| p-I | 6u | 3.6 | 27 ± 1 | 2.3 ± 0.2 | 12 ± 1 |
| m-I | 2r | 4.8 | 24 ± 2 [d] | 0.9 ± 0.1 [d] | 26 ± 3 [d] |
| p-I | 2s | 4.9 | 17 ± 3 [d] | 1.4 ± 0.4 [d] | 12 ± 4 [d] |
| o-CH ₂ OH | 9a | 1.0 | NR [f] | NR [f] | NR [f] |
| m-CH ₂ OH | 9b | 0.9 | 44 ± 1 | 4.0 ± 0.2 | 10 ± 2 |
| p-CH ₂ OH | 9c | 0.8 | 115 ± 6 | 8.0 ± 0.6 | 14 ± 3 |
| o-MeO | 2t | 4.1 | 8.8 ± 0.9 [d] | 0.9 ± 0.2 [d] | 9.3 ± 0.6 [d] |
| m-MeO | 2u | 3.3 | 53 ± 5 [d] | 4.3 ± 0.6 [d] | 12 ± 2 [d] |
| p-MeO | 2v | 3 | 140 ± 40 [d] | 30 ± 10 [d] | 5 ± 2 [d] |
| o-Et | 6v | 4.0 | 11 ± 1 | 2.5 ± 0.4 | 4 ± 1 |
| m-Et | 6w | 5.5 | 17 ± 0.7 | 2.1 ± 0.2 | 8 ± 1 |
| p-Et | 6x | 5.1 | 28 ± 0.8 | 4.4 ± 0.3 | 6 ± 1 |
| o-Et | 2w | 4.8 | 17 ± 2 [d] | 7 ± 1 [d] | 2.4 ± 0.6 [d] |
| m-Et | 2x | 4.6 | 8 ± 2 [d] | 3.8 ± 0.8 [d] | 2.1 ± 0.1 [d] |
| m-CF ₃ O | 6y | 5.1 | 3 ± 0.2 | 0.3 ± 0.01 | 11 ± 2 |
| p-CF ₃ O | 6z | 5.1 | 16 ± 0.3 | 1.3 ± 0.1 | 12 ± 2 |
| m-CF ₃ O | 2aa | 4.9 | 40 ± 10 [d] | 2.3 ± 0.6 [d] | 19 ± 1 [d] |
| p-CF ₃ O | 2ab | 4.9 | 27 ± 6 [d] | 3.1 ± 0.9 [d] | 8.7 ± 0.3 [d] |
| m-iPr | 6aa | 6.7 | 21 ± 0.5 | 1.9 ± 0.1 | 11 ± 1 |

| R-group and position on ring [a] | Compound number | Apparent logP [b] | apparent $k_{cat} [c] (s^{-1}) \times 10^{-2}$ | apparent $K_m^{dms-GCVLS} [c] (\mu M)$ | apparent $k_{cat}/K_m^{dms-GCVLS} [c] (\mu M^{-1} s^{-1}) \times 10^{-2}$ |
|----------------------------------|-----------------|-------------------|--|--|---|
| p-iPr | 6ab | 6.8 | 44 ± 5 | 2.14 ± 2.9 | 2 ± 1 |
| o-Ph | 6ac | Nde [e] | NR [f] | NR [f] | NR [f] |
| p-Bn | 6ad | 6.5 | 30 ± 0.6 | 2.3 ± 0.1 | 13 ± 3 |

[a] The analogues are listed in order of increasing substituent surface area.

[b] LogP measurements of the corresponding alcohol.

[c] $app k_{cat}$, $app K_m^{peptide}$ and apparent $k_{cat}/K_m^{peptide}$ were determined using a Michaelis-Menton analysis as described. [32]

[d] From Troutman et al. [32]

[e] Nde indicates not determined.

[f] NR indicates no reaction determined by RP-HPLC product analysis.